

Frozen shuffle update for an asymmetric exclusion process with open boundary conditions

C. Appert-Rolland, J. Cividini, and H.J. Hilhorst

1 - University Paris-Sud; Laboratory of Theoretical Physics
Bâtiment 210, F-91405 ORSAY Cedex, France.

2 - CNRS; UMR 8627; LPT
Bâtiment 210, F-91405 ORSAY Cedex, France.

E-mail: Cecile.Appert-Rolland@th.u-psud.fr,
Julien.Cividini@th.u-psud.fr, Henk.Hilhorst@th.u-psud.fr

Abstract. We introduce a new update algorithm for exclusion processes, more suitable for the modeling of pedestrian traffic. Pedestrians are modeled as hard-core particles hopping on a discrete lattice, and are updated in a fixed order, determined by a *phase* attached to each pedestrian. While the case of periodic boundary conditions was studied in a companion paper, we consider here the case of open boundary conditions. The full phase diagram is predicted analytically and exhibits a transition between a free flow phase and a jammed phase. The density profile is predicted in the frame of a domain wall theory, and compared to Monte Carlo simulations, in particular in the vicinity of the transition.

Keywords: pedestrian traffic, exclusion process, shuffle update, boundary driven phase transition

1. Introduction

As part of the effort to describe pedestrian motion, the past years have seen the development of cellular automata based models, among which the so-called ‘floor field’ model [1, 2]. These models represent pedestrians as particles that jump from site to site on a discrete lattice, with an exclusion principle that forbids two pedestrians to simultaneously occupy the same site. In general, the pedestrians’ positions are subject to a parallel update procedure, *i.e.*, the particles attempt to jump at the same instants of time. Although this type of update ensures a quite regular motion under free flow conditions, it creates conflicts when two or more pedestrians try to move at the same time to the same target site.

Introducing an arbitrary numerical decision procedure to resolve these conflicts can be considered as a drawback and alternative update procedures have been looked for. In reference [4], for example, large pedestrian simulations are performed by means of a random shuffle update. In this sequential update scheme an updating order for the pedestrians is drawn at random at the beginning of each time step.

The random shuffle update was first proposed and studied in [5, 6, 7]. It was applied there to the Totally Asymmetric Simple Exclusion Process (TASEP), which can be seen as a basic model for pedestrian traffic. More generally, exclusion processes are archetypes of out-of-equilibrium systems and have been used to model various transport phenomena, including road and intracellular traffic, or ant motion [8].

Here and in a companion paper [9] we introduce a new variant of the shuffle update called the *frozen shuffle update*. Under this updating procedure each particle i is assigned, either at the beginning of the simulation or when it enters the system, a random *phase* $\tau_i \in [0, 1)$. In each time step particles are updated in the order of increasing phases. The phases may be thought of as the phases in the walking cycle, where one pedestrian may be slightly in advance with respect to another one. This advance then determines who passes first in case of conflict.

We have recently studied the frozen shuffle update for the TASEP on a ring, *i.e.* on a closed system [9]. This system is appropriately described by its current J as a function of the particle density ρ . We found [9] that the TASEP on a ring undergoes a phase transition at a critical density $\rho = \frac{2}{3}$, where $J(\rho)$ attains its maximum through a linear cusp. The critical point separates a ‘free flow’ phase from a ‘jammed’ phase.

In the present paper we study an open-ended TASEP with frozen shuffle update. Whenever a new particle, say i , enters through the open boundary, its place in the updating order is specified by a newly drawn τ_i . It will then keep this same τ_i until it leaves the system. In section 2 we define the frozen shuffle update. We will consider only its deterministic version in which allowed jumps are carried out with probability one. In addition to the bulk rules of motion, which are the same as on the ring [9],

we specify in section 3 the rules by which particles enter and leave the system. This procedure will depend on two additional parameters, an entrance probability α and an exit probability β . In section 4 the phase diagram of the system in the $\alpha\beta$ plane will be determined analytically. We find a transition line $\alpha = \beta$ between, again, a free flow and a jammed phase. The bulk particle density $\rho(\alpha, \beta)$ and the current $J(\alpha, \beta)$ are determined analytically and appear in excellent agreement with simulations. In section 5 the finite size effects, in particular near the transition line, are described by a domain wall approach.

2. Frozen shuffle update for the 1D TASEP

2.1. Frozen shuffle update

We consider a system of hard-core particles (*i.e.* at most one per lattice site) on a one-dimensional lattice of L sites numbered from left to right by $k = 1, 2, \dots, L$. The particles enter the system at $k = 1$, make hops of a single lattice distance to the right, and leave the system at $k = L$. The hops are executed according to the following *frozen shuffle* update scheme. A particle i , when it enters the system, is assigned a random phase $\tau_i \in [0, 1)$, which it keeps until it leaves the system. The phases are drawn from a predefined distribution. In each time step all particles are updated (*i.e.* attempt to hop one step to the right) in the order of increasing phases. An attempted hop is successful if and only if the target site is empty.

Throughout, the variable t will stand for continuous time; time steps will be indicated by integer values $t = 0, 1, \dots, s, \dots$. The particle configuration at time $t = s$ is considered to be the result of the s th time step.

2.2. Two stable bulk states

In recent work [9] we have identified two distinct stable bulk states sustained by this update scheme. In an infinite homogeneous system these may be discussed without reference to boundary conditions. They are the *free flow* state and the *jammed* state.

Free flow state. In the free flow state all particles are able to move forward at each time step. Hence they all have a velocity $v = 1$, that is, one lattice distance per time step. The current $J^F = \rho v$ in the free flow state is therefore in these units given by

$$J^F = \rho. \tag{1}$$

The technical definition is that *the system is in a free flow state if whenever two adjacent lattice sites are occupied by particles, the particle to the right has the lower phase.*

Jammed state. The second stable bulk state is the *jammed* state. This is a highly compacted state of a special kind. Technically, *the system is in the jammed state if,*

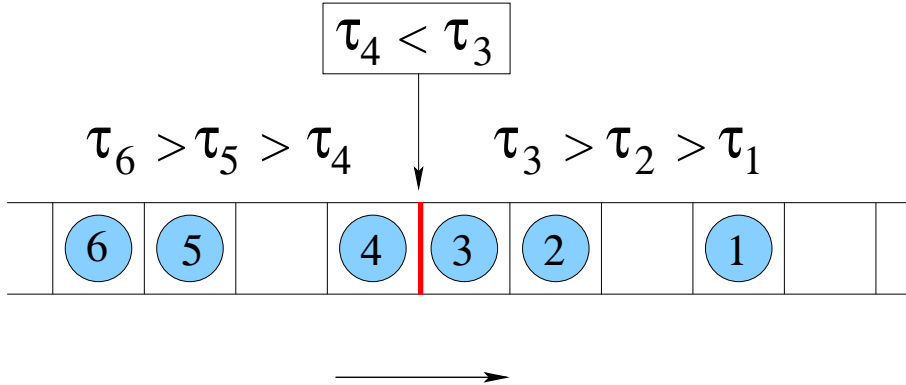


Figure 1. Six hard-core particles on a one-dimensional lattice whose sites are represented by square boxes. The arrow indicates the hopping direction. Our convention will be to place a heavy (red) vertical bar to the left of each particle that has a larger phase than its follower (in the present example, particle 3). The configuration shown is not a free flow state, since the particle pair (3, 4) violates the free flow condition; particle 4 is unable to move during the upcoming time step. The configuration is not a jammed state either, since the holes between the particle pairs (1, 2) or (4, 5) violate the jammed state condition.

whenever a particle has a smaller (larger) phase than its follower, then it is located on the site immediately to the right of its follower (is separated from its follower by at most a single hole). As a consequence, in this state, a fraction of the particles remains blocked at each time step; the average particle velocity therefore is less than unity.

Stability. The conditions for the free flow state and the jammed state are illustrated by figure 1. It is tacitly understood that these conditions are to be evaluated after completion of a full time step. There exist many particle configurations that are neither free flow nor jammed states[‡]. For a system on a ring lattice the latter two were shown [9] to be attractors in phase space toward which arbitrary initial states evolve. They are stable in the sense that once the system has entered one of them, it will stay in it.

Platoons. We now look for the counterpart in the jammed phase of the current-density relation (1). The flow in the jammed state is most easily discussed in terms of platoons. A *platoon* is a succession of particles occupying consecutive sites and having increasing phases; the first particle of a platoon having a lower phase than the particle that precedes it; and the last particle of a platoon having a higher phase than the particle that follows it. It was shown [9] that in the jammed phase each particle belongs

[‡] There also exists a small class of configurations that are, technically, both ‘free flow’ and ‘jammed’, namely the configurations in which *each* platoon is preceded by a hole; this fact is of little consequence for the discussion.

to a platoon.

Frozen shuffle update leads to simple platoon dynamics. A platoon moves as a whole, *i.e.*, if its first particle can move, then in the same time step the whole platoon will move one lattice distance to the right. Equivalently, one may say that the hole initially in front of the platoon has hopped across it to the left over a distance equal to the platoon length (as will be further illustrated in section 3.4). This allows us to make the following statement [9]. Let ν be the average platoon length in some suitable spatially homogeneous statistical ensemble. Since the hole density is $1 - \rho$, and since only platoons that have a hole in front of them can move, the current J^J in a jammed phase is given by

$$J^J = \nu(1 - \rho), \quad (2)$$

which is the relation that we looked for. Henceforth the superscripts J and F will indicate quantities referring to the jammed and the free flow state, respectively.

As the final comment of this section we remark that expressions (1) and (2) refer to spatially homogeneous states of, in principle, infinite extent. Our interest below will be in a finite system with boundary conditions specified by two parameters α and β . In the next section we define these boundary conditions and express the stationary state current $J(\alpha, \beta)$ of this finite system in terms of the currents J^F and J^J discussed above.

3. Rules for entering and exiting

3.1. Entering rule

The rule governing the entering of particles into the system is motivated by an equivalent hard rod description [9] of the system in the free flow state[§]: Let nonoverlapping rods of unit length, as shown in figure 2, move in continuous time at constant speed $v = 1$ along the x axis. At any integer instant of time s , each rod i will cover exactly one integer spatial coordinate $x = k$. We will say that at time step s the particle i associated with the rod i occupies lattice site k in the corresponding discrete model. This particle i will then be on lattice site $k + 1$ at time $s + 1$, and so on. The (noninteger) time $s + \tau_i$ at which rod i uncovers position k and starts to cover position $k + 1$ defines the phase τ_i of particle i in the discrete model.

If the rods are (at any instant of time) uniformly distributed in space, subject only to the no-overlap constraint, then the intervals T_i between them (see figure 2) are independent variables drawn from an exponential distribution

$$P(T) = ae^{-aT}, \quad T \geq 0. \quad (3)$$

where a is a positive parameter.

[§] This equivalence breaks down when there is jamming, as it would lead to overlapping rods.

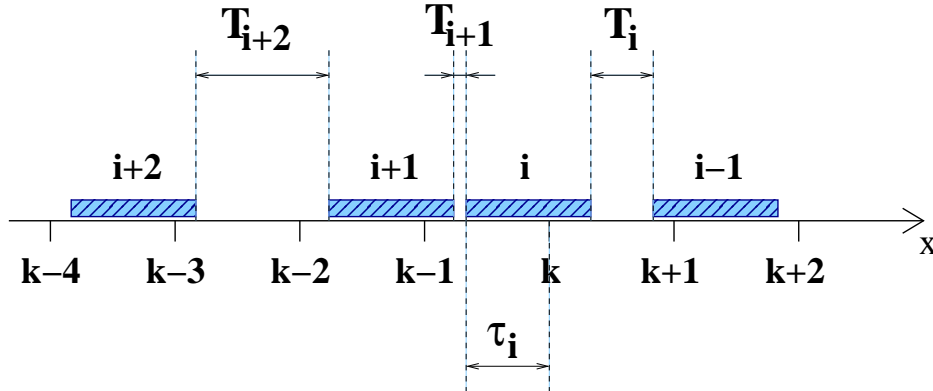


Figure 2. Rods move at constant speed $v = 1$ from left to right along the x axis. The time interval between the tail of the i th and the head of the $(i + 1)$ th rod is called T_i . The T_i are drawn randomly from the exponential distribution (3). We have also represented the underlying discrete lattice, that allows to define the mapping between the continuous and the discrete model. If the snapshot is taken at an integer time s , then the phase τ_i of particle i in the discrete model corresponds in the continuous model to the distance between the tail of rod i and the integer position k that rod i overlaps (since $v = 1$, time and space may be identified).

The equivalence between the rod and the particle motion lead us to adopt the following rule for particles entering the lattice, in order to have the same time interval distribution between particles in the discrete system. A particle can be injected from the exterior onto the first lattice site (labeled 1) only if that site is empty. If site 1 gets emptied at some instant of time $s + \tau_{i-1}$ (due to particle $i - 1$ moving forward to site 2), then it will be reoccupied by a new particle i at a random time $t_i = s + \tau_{i-1} + T_i$ with T_i distributed according to (3). This new particle will therefore have a phase τ_i given by the recurrence relation

$$\begin{aligned} \tau_i &= t_i \bmod 1 \\ &= (\tau_{i-1} + T_i) \bmod 1, \end{aligned} \tag{4}$$

to which we will return in section 3.

Below it will sometimes be convenient to use the probability, to be called α , that the initial site, when empty at some arbitrary (real) instant of time t , is occupied at time $t + 1$. This quantity is independent of t and with (3) it follows that

$$\begin{aligned} \alpha &= \text{Prob}\{T < 1\} \\ &= 1 - e^{-a}. \end{aligned} \tag{5}$$

We will refer to a and α as the ‘entrance rate’ and ‘entrance probability’, respectively.

3.2. Entering current

Let ρ^F and J^F denote the spatial density and the current, respectively, of the incoming particles under free flow conditions. They then satisfy the free flow relation (1), that is, $J^F = \rho^F$. We now express these quantities in terms of the parameter a . Let T_N^{in} be the time needed for N particles $i = 1, 2, \dots, N$ to enter the system. Then T_N^{in} is the sum of the time intervals T_i and, for each particle, of a unit time interval during which it blocks the access of a new particle to site 1. In the limit $N \rightarrow \infty$ the stochastic variable T_N^{in} becomes sharply peaked around its average, that is,

$$\lim_{N \rightarrow \infty} \frac{T_N^{\text{in}}}{N} = \lim_{N \rightarrow \infty} \frac{1}{N} \sum_{i=1}^N (T_i + 1) = \overline{T_i} + 1 = \frac{1}{a} + 1. \quad (6)$$

Since $J^F = \lim_{N \rightarrow \infty} N/T_N^{\text{in}}$, it follows that at the left hand end of the lattice we have, *under free flow entrance conditions*,

$$J^F = \frac{a}{1+a}, \quad \rho^F = \frac{a}{1+a}. \quad (7)$$

The injection procedure seeks therefore to impose onto the system a free flow state with a density and current (7) characterized by the parameter a (or α). This free flow is interrupted only when a particle meets with an obstacle: that might be a barrier at the exit point or a jam caused by other particles anywhere in the interior of the system. In the special case that site 1 is occupied by a particle which is itself blocked, the entering rule of section 3.1 still applies, but in that case the free inflow stops. Before commenting further we will now examine what happens at the exit point.

3.3. Exiting rule

We choose to adopt the following rule for particles leaving the system. If the last lattice site, labeled L , is occupied by a particle i with phase τ_i , then, at each instant of time $s + \tau_i$, particle i leaves the system with probability β and stays on site L with probability $1 - \beta$. For $\beta = 1$ the free flow is unimpeded at the exit. However, when $\beta < 1$, the free flow will at times be randomly impeded, which may create a slowly advancing waiting line for the particles near the exit. When the rear end of this waiting line propagates all the way backward to the entrance, the system is in its jammed state. Below we will investigate the conditions for this to happen.

3.4. Exiting current

Let the particles near the exit point be in a jammed state configuration and let ρ^J and J^J denote their density and their current, respectively, under this condition. These two quantities then satisfy the jammed state relation (2), that is, $J^J = \nu(1 - \rho^J)$. We will now show how they are determined by the parameters β and α .

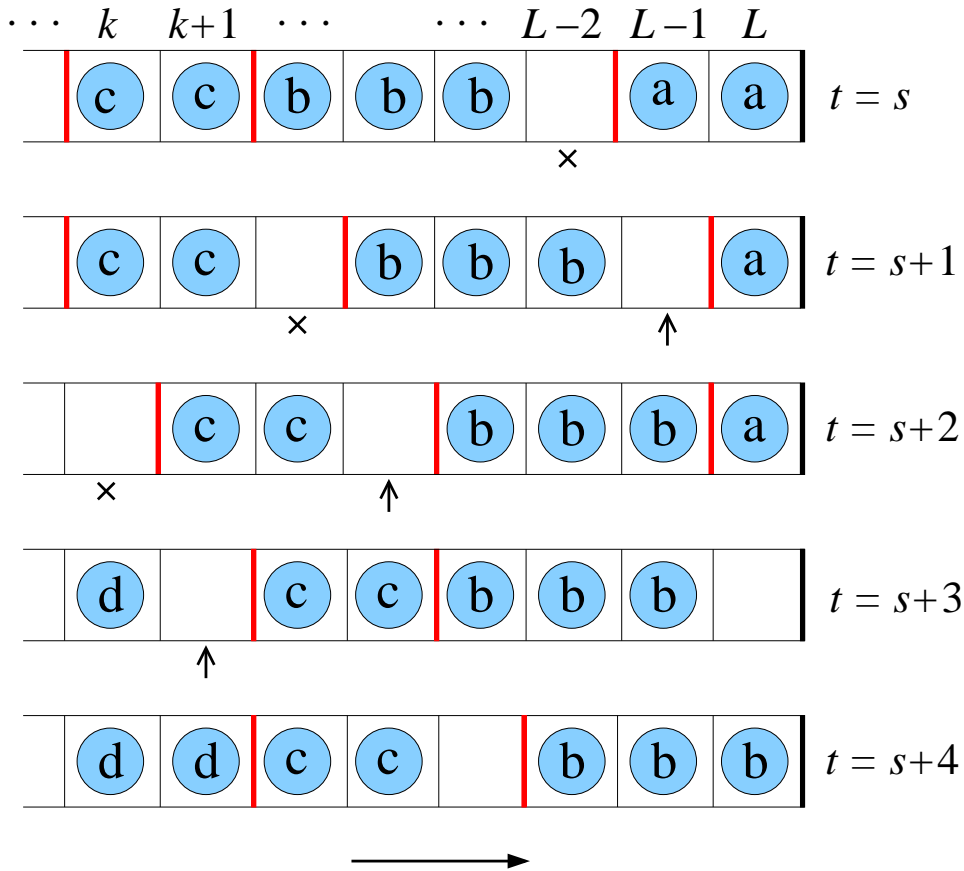


Figure 3. The lattice near the exit site L , shown at five successive time steps (s is an arbitrary integer). Particles in the same platoon are labeled by the same letter; their phases, not indicated, increase towards the left. A heavy (red) bar indicates an end-of-platoon. The particles are in a jammed state (platoons are separated by at most a single hole). The particle motion is deterministic except for the exit from site L , which takes place only with probability β . Time step $t = s$: Initial configuration. Time step $t = s + 1$: The particle heading platoon a exits and its follower hops to the exit site. A new hole, marked by an up-arrow \uparrow , enters the system from the right. Besides, platoon b advances by a position exchange with the hole marked by a cross \times . Platoon c is blocked. Time step $t = s + 2$: Particle a , subject to the random exit rule, stays on site L . Platoons b and c advance. The two marked holes exchange positions with the platoon to their left. Time step $t = s + 3$: The last particle of platoon a leaves the system and is replaced with a new hole on site L . Platoon b is blocked but c and d move ahead. Time step $s = t + 4$: Platoons b and d move ahead, but c is blocked.

We reason as follows. A particle on site L has at each time step a probability β to leave the system. The probability q_r that it exit at the r th time step is $q_r = (1 - \beta)^{r-1}\beta$, so that for leaving the system it needs an average number of time steps equal to $\sum_{r=1}^{\infty} r q_r = \beta^{-1}$. In the jammed state the particle configuration consists of platoons. An example is shown in figure 3, where the last particle of each platoon is indicated by a heavy (red) vertical bar to its left.

When the particle on site L exits, the whole platoon that it was heading advances one step, so that site L is occupied by the next particle in the exiting platoon. When the last particle of a platoon has left the system, site L is unoccupied and remains so during one time step, after which it is occupied by the first particle of the next platoon. Therefore, the average number of time steps needed for an n -particle platoon to exit, counted from the moment that its first particle arrives on site L until the moment that the next platoon's first particle arrives there, is equal to $n\beta^{-1} + 1$. If ν is the average platoon length, then $\nu\beta^{-1} + 1$ is the average time needed for ν particles to exit the system. At the right hand end of the lattice we therefore have, *under jammed flow exit conditions*,

$$J^J = \frac{\nu\beta}{\nu + \beta}, \quad \rho^J = \frac{\nu}{\nu + \beta}. \quad (8)$$

Before combining our analyses of the entrance and the exit points we complete this section by finding an expression for the mean platoon length ν , appearing in (8). It should be noticed that ν is completely determined by the injection procedure. Actually we shall see that it can be expressed as a function of α .

3.5. Expression for $\nu(\alpha)$

The average platoon length ν depends on the injection procedure defined in section 3.1, and in particular on the way the phases τ_i are assigned. Let τ_0 be some arbitrary initial phase. The phases τ_i are then related to the time intervals T_j by

$$\begin{aligned} \tau_i &= \left[\tau_0 + \sum_{j=1}^i (T_j + 1) \right] \bmod 1, \quad i = 1, 2, \dots, \\ \tau_i &= \left[\tau_0 + \sum_{j=1}^i \hat{T}_j \right] \bmod 1 \end{aligned} \quad (9)$$

where we set

$$\hat{T}_j \equiv T_j \bmod 1. \quad (10)$$

The probability distribution \hat{P} for the \hat{T}_j may be calculated as

$$\hat{P}(\hat{T}) = \int_0^{\infty} dT P(T) \delta(\hat{T} - T \bmod 1)$$

$$\begin{aligned}
&= \sum_{m=-\infty}^{\infty} \int_0^{\infty} dT a e^{-aT} \delta(\hat{T} - T + m) \\
&= \sum_{m=-\infty}^{\infty} a e^{-a(\hat{T}+m)} \theta(\hat{T} + m),
\end{aligned} \tag{11}$$

in which $\theta(x)$ is the Heaviside step function, here defined by $\theta(x) = 0$ for $x < 0$ and $\theta(x) = 1$ for $x \geq 0$. Substituting for $\theta(x)$ its definition in (11) restricts the sum, which can then be calculated as follows

$$\begin{aligned}
\hat{P}(\hat{T}) &= \sum_{m=0}^{\infty} a e^{-a(\hat{T}+m)} \\
&= \frac{a}{1 - e^{-a}} e^{-a\hat{T}}, \quad 0 \leq \hat{T} < 1.
\end{aligned} \tag{12}$$

A useful intermediate step is to rewrite (9) as

$$\tau_i = \hat{\tau}_i \bmod 1 \tag{13}$$

with

$$\hat{\tau}_i = \tau_0 + \sum_{j=1}^i \hat{T}_j. \tag{14}$$

The $\hat{\tau}_i$ are a sequence of random points on the positive $\hat{\tau}$ axis, not confined to $[0,1)$, and there is at least one point in every interval between two integers k and $k+1$. If $\hat{\tau}_i$ and $\hat{\tau}_{i+1}$ are in the same interval $[k, k+1)$, then the corresponding τ_i and τ_{i+1} verify $\tau_i < \tau_{i+1}$ after the modulo in (13). If $\hat{\tau}_i$ lies in $[k, k+1)$ and $\hat{\tau}_{i+1}$ in $[k+1, k+2)$, then recalling that $\hat{T}_{i+1} < 1$, we have $\tau_i > \tau_{i+1}$. Thus each set of $\hat{\tau}_i$ values within an interval $[k, k+1)$ will give one platoon in the jammed phase. The average platoon length ν is therefore equal to the average number of $\hat{\tau}_i$ values in a unit interval on the $\hat{\tau}$ axis, which in turn is the inverse of the average length of the modulo 1 time intervals \hat{T}_j . From (12) we now obtain easily

$$\begin{aligned}
\frac{1}{\nu} &= \int_0^1 d\hat{T} \hat{T} \hat{P}(\hat{T}) \\
&= 1 + \frac{1}{a} - \frac{1}{1 - e^{-a}},
\end{aligned} \tag{15}$$

which is the desired expression for ν in terms of a , or equivalently, α .

Upon combining (15) with (8) we find that the exiting current J^J may be expressed as

$$\begin{aligned}
J^J(\alpha, \beta) &= \beta \left[1 + \frac{\beta}{\nu} \right]^{-1} \\
&= \frac{\beta}{1 + \beta \left(\frac{1+a}{a} \right) - \left(\frac{\beta}{\alpha} \right)}
\end{aligned}$$

$$= \frac{1}{\frac{1+a}{a} + \frac{1}{\beta} - \frac{1}{\alpha}}. \quad (16)$$

We remark that rewritings like the one above are carried out most efficiently by working with a and α as though they were unrelated variables.

This completes the necessary preliminaries. Everything is in place now for us to determine the phase diagram of the system subject to the boundary conditions (α, β) .

4. Phase diagram

In the previous sections, we have identified and characterized two possible stationary states, free flow and jammed. It is clear that the free flow state cannot be sustained if the outflow predicted by (16) is smaller than the inflow given by (7); in that case the jamming will propagate across the system from exit to entrance. Inversely, it is also clear that the jammed flow state requires the outflow, given by (16), to be smaller than the inflow (7). Hence in the stationary state viewed as a function of α and β we expect the occurrence of a phase transition on the line

$$J^F(\alpha) = J^J(\alpha, \beta), \quad (17)$$

where we have indicated explicitly the dependence of the currents on the two model parameters α and β . It is interesting to notice that (16) may be rewritten as

$$\frac{1}{J^J} = \frac{1}{J^F} + \frac{1}{\beta} - \frac{1}{\alpha} \quad (18)$$

Then one immediately finds the critical line $J^F = J^J$ in the $\alpha\beta$ plane is

$$\alpha = \beta. \quad (19)$$

This simple result would have been rather unsurprising in the case of particle/hole symmetry. However, in the present case the particle/hole symmetry is broken by the update scheme, and we have not found a simpler derivation of (19) than the one given above.

As a consequence of (19) we have for the current $J(\alpha, \beta)$ carried by the system in its stationary state

$$J(\alpha, \beta) = \begin{cases} J^F(\alpha), & \alpha \leq \beta, \\ J^J(\alpha, \beta), & \alpha \geq \beta, \end{cases} \quad (20)$$

and

$$\rho(\alpha, \beta) = \begin{cases} \rho^F(\alpha), & \alpha < \beta, \\ \rho^J(\alpha, \beta), & \alpha > \beta, \end{cases} \quad (21)$$

with J^F and ρ^F given by (7) and J^J and $\rho^J = J^J/\beta$ by (16). Across the critical line the current is continuous and the particle density jumps by a factor β ,

$$J_c^J = J_c^J, \quad \rho_c^J = \beta \rho_c^F, \quad (22)$$

where the subscript ‘c’ indicates evaluation on the critical line. This jump is a true discontinuity only in the limit $L \rightarrow \infty$. Finite size rounding will be described in the next section.

The closing remarks of this section concern the similarities and differences that appear here between the present frozen shuffle update scheme and other schemes applied to the TASEP. First, we note that the critical line (19) obtained here for the TASEP is identical to the one found with other update schemes, whether it be random sequential update [10, 11], parallel update [12], or ordered sequential update [13]. Secondly, however, our expressions for J^F and J^J are specific to the update procedure adopted here. In particular, it is remarkable that in the present case the jammed phase current depends not only on β but also, through the mean platoon length $\nu(\alpha)$, on the entrance probability α . Indeed, the jammed phase dynamics is completely determined by the platoon structure, which in turn results from the injection procedure - whatever this procedure may be.

Thirdly, the frozen shuffle update of this paper, unlike the other updates, does not lead to a ‘maximal current’ phase: here the current is always equal to either J^F or J^J , that is, always fixed by the boundary conditions. This feature, confirmed by simulations, is due to the deterministic character of the TASEP considered here: when a particle has the possibility to hop forward, it does so with probability 1.

5. Domain wall picture

5.1. Microscopic domain wall position

If $\beta < 1$, a waiting line may be formed at the exit whose rear end is nothing but a domain wall separating a spatial region with free flow from one with jammed flow. For $\alpha < \beta$ the system is in the free flow phase; the incursions of the jammed region into the system, starting from the exit point, will not exceed some finite localization length and be short-lived. Hence the domain wall is localized near the exit point. For $\alpha > \beta$ the system is in the jammed phase; the waiting line invades the whole system and the domain wall is localized near the point of entry. For $\alpha \approx \beta$ the domain wall position is subject to large fluctuations that we will study below; for $\alpha = \beta$ it is completely delocalized.

The frozen shuffle update of the TASEP offers the advantage, compared to previously studied update schemes, that the wall position may be defined very accurately, namely on a microscopic scale^{||}. Since in the free flow state no particle is blocked at any time, it is natural to say that the domain wall position is determined by the leftmost particle ever to have been blocked during an attempted move. By

^{||} A similar microscopic definition could be given for a parallel update with deterministic dynamics.

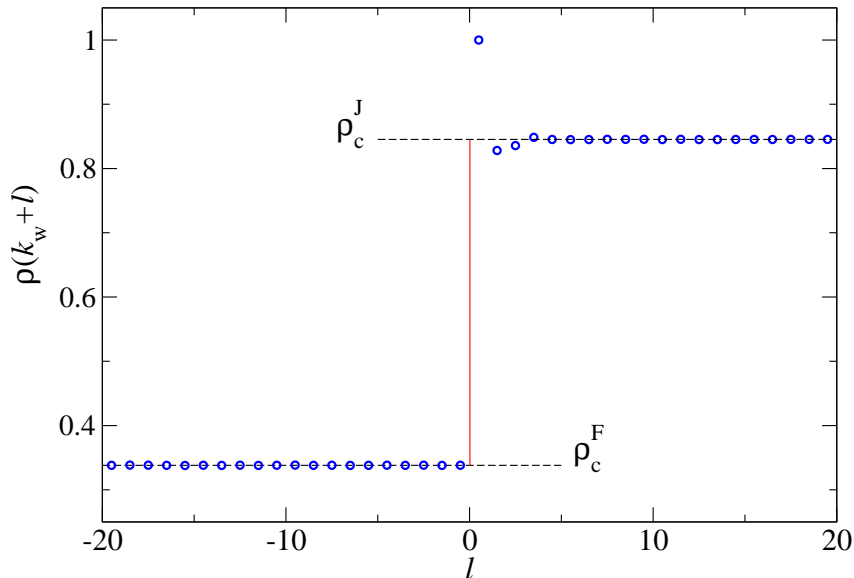


Figure 4. Density profile $\rho(k_w + l)$ in the coordinate system attached to the domain wall; l is the distance to the fluctuating wall position k_w . The data were taken on the critical line with $\alpha = \beta = 0.4$. The profile is very close to a step function that jumps from ρ_c^J to ρ_c^F at the vertical (red) line. Only in the jammed state does there appear some structure on the scale of a few lattice distances.

convention we will take for the domain wall position k_w the half-integer coordinate of the link on the left of this leftmost blocked particle. When the leftmost blocked particle moves again, it carries the wall along; when another particle positioned to its left is prevented to move, the wall position is transferred to the link on the left of that particle. All particles to the left of the wall position are in the free flow state and all those to its right are in the jammed state, in the sense of the definitions of section 2.2. There is no need to develop tracking strategies as was necessary [14], for example, for the TASEP with random sequential update.

Let $\rho(k)$ be the site dependent particle density. Figure 4 shows our simulation results for the profile in the reference system of the wall, within an environment of 20 lattice distances around k_w . Data were taken only when the wall was more than 20 lattice units away from both ends. By construction $\rho(k_w + \frac{1}{2}) = 1$. Apart from this exceptional site the density profile is almost a step function, separating flat density profiles with densities ρ^F and ρ^J , as shown by the vertical (red) line in figure 4. Only on the high density side of the wall does there appear some structure, restricted to a microscopic distance of the order of a platoon length (equal to $\nu(0.4) = 2.18$ in the case of figure 4).

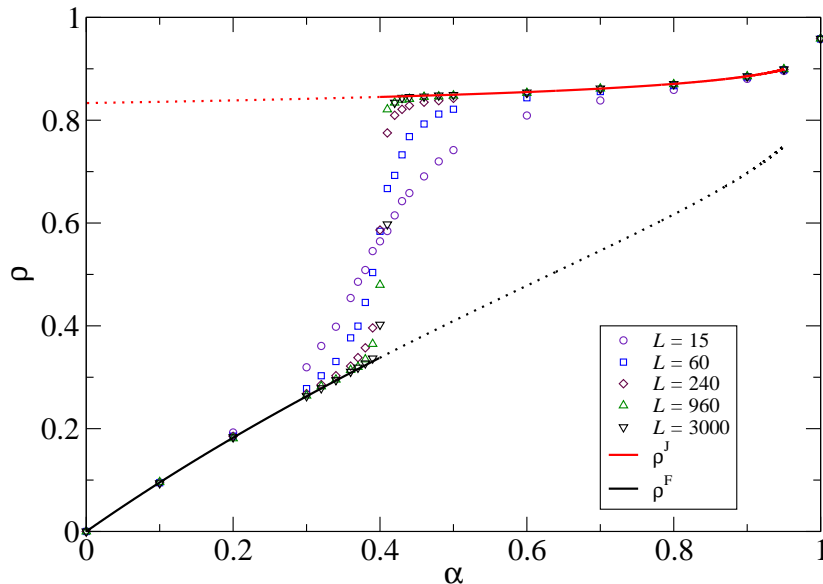


Figure 5. Space averaged particle density ρ versus entrance probability α for the open-ended chain with exit probability $\beta = 0.4$. The simulation data are for a sequence of increasing system sizes. They converge towards the lower (black) and upper (red) solid curves, which are the theoretical densities $\rho^F(\alpha)$ and $\rho^J(\alpha, \beta)$ of equations (31) and (32). The dotted curves are their metastable extensions. At the critical value $\alpha = \alpha_c = 0.4$ the density jumps from its free flow value ρ_c^J to its jammed flow value ρ_c^F . The simulation data for finite system sizes L , however, show strong finite size rounding.

5.2. Domain wall theory

The strong fluctuations of the wall position near criticality give rise to large finite size effects visible on the physical observables. One of these is the spatially averaged density, still denoted ρ , in a finite system. Simulation data for this quantity are shown in figure 5 and are seen to converge only slowly to the discontinuous theoretical curve. Below, a description of the system dynamics in terms of the wall motion will allow us to account for such finite size effects.

Let $Q_k(t)$ be the probability for the wall to be located at $k_w = k + \frac{1}{2}$, *i.e.* on link $(k, k+1)$, where we may take $k = 0, 1, \dots, L$. The “links” $(0, 1)$ and $(L, L+1)$ are virtual; $Q_0(t)$ is the probability that the leftmost blocked particle occupies position $k = 1$ and $Q_L(t)$ is the probability that none of the particles present in the system at time t has ever been blocked. We will follow here the mesoscopic approach to domain wall motion that was earlier applied with success to the TASEP with other update schemes [15, 16] and that has been able to predict stationary and nonstationary [17, 18, 19] features of those TASEP versions. According to this approach we hypothesize that

(i) the probability $Q_k(t)$ obeys the master equation for an asymmetric simple random walk,

$$\frac{d}{dt}Q_k(t) = D_+ [Q_{k-1}(t) - Q_k(t)] + D_- [Q_{k+1}(t) - Q_k(t)], \quad (23)$$

for $k = 0, 1, 2, \dots, L$ with the reflecting boundary conditions $D_+Q_{-1} = D_-Q_0$ and $D_-Q_{L+1} = D_+Q_L$; and

(ii) the coefficients D_{\pm} in this equation are related to the currents and the densities in the two phases by

$$D_+ = \frac{J^J}{\rho^J - \rho^F}, \quad D_- = \frac{J^F}{\rho^J - \rho^F}. \quad (24)$$

For the present case of frozen shuffle update the validity of equations (23) and (24) has not been demonstrated on the basis of first principles¶. We must therefore consider that they provide an approximate description.

5.3. Continuous description

Equation (23) is easily studied on a discrete lattice. However, when the wall position fluctuates on the scale of many lattice distances (which it will do close to the critical line $\alpha = \beta$), we may replace the index k by a continuous variable $0 \leq k \leq L$. We will write $Q(k, t)$ instead of $Q_k(t)$ to indicate that we have performed this operation. Equation (23) then becomes the Fokker-Planck equation

$$\frac{\partial Q(k, t)}{\partial t} = -\delta \frac{\partial Q}{\partial k} + D \frac{\partial^2 Q}{\partial k^2}, \quad (25)$$

in which

$$\delta = D_+ - D_-, \quad D = \frac{1}{2}(D_+ + D_-) \quad (26)$$

appear as the drift velocity and the diffusion constant, respectively, of the domain wall. The boundary conditions become $\partial Q(k, t)/\partial k = Q(k, t)/\xi$ for $k = 0, L$. Subject to these, and if we set $\xi = D/\delta$, the stationary solution of (25) is

$$Q_{\text{st}}(k) = \frac{e^{k/\xi}}{\xi(e^{L/\xi} - 1)}, \quad 0 \leq k \leq L. \quad (27)$$

For ξ positive (negative) the wall is localized near $k = L$ (near $k = 0$), as anticipated; moreover, the domain wall theory gives for the localization length $|\xi|$ the explicit expression

$$\xi = \frac{J^J + J^F}{2(J^J - J^F)} = \frac{2 - J^F \left(\frac{1}{\alpha} - \frac{1}{\beta} \right)}{2J^F \left(\frac{1}{\alpha} - \frac{1}{\beta} \right)} \quad (28)$$

¶ That is, starting from the master equation that defines the time evolution of the particle configurations.

where the second expression was derived with the aid of (18).

Let $\rho_L(k)$ denote the particle density at k averaged over the domain wall fluctuations; we will refer to this function as the ‘density profile’. The domain wall theory gives for the density profile the following analytic expression,

$$\rho_L(k) = \rho^J \int_0^k dk' Q_{\text{st}}(k') + \rho^F \int_k^L dk' Q_{\text{st}}(k'). \quad (29)$$

Working this out with the aid of (27) we find

$$\rho_L(k) = \rho^J + (\rho^F - \rho^J) \frac{1 - e^{-(L-k)/\xi}}{1 - e^{-L/\xi}} \quad (30)$$

which is valid for $L \gg 1$ and k of order L (as we used (27)) and represents an exponential profile connecting $\rho(0) = \rho^F$ at $k = 0$ to $\rho(L) = \rho^J$ at $k = L$. We recall that

$$\rho^F = \frac{a}{1+a}, \quad (31)$$

$$\rho^J = \frac{1}{\beta \left(\frac{1}{\rho^F} + \frac{1}{\beta} - \frac{1}{\alpha} \right)} \quad (32)$$

Equation (28) shows that if we vary α (hence a) at fixed β , the localization length $|\xi|$ diverges at the critical value $\alpha = \alpha_c = \beta$. Exactly on the critical line $\alpha = \beta$, the wall position distribution (27) becomes flat, *i.e.*, $Q_{\text{st}}(k) = 1/L$, the densities on each side of the wall are related by $\rho^J = \rho^F/\alpha_c$, and concomitantly the profile (35) becomes the straight line

$$\rho_L(k) = \frac{a_c}{1+a_c} \left[1 + \frac{1 - \alpha_c k}{\alpha_c L} \right], \quad (33)$$

where $1 - e^{-a_c} \equiv \alpha_c$.

In figure 6 we show, for a system of length $L = 302$, for β fixed and for various values of α around $\alpha_c = \beta$, the theoretical density profiles $\rho_L(k)$ based on equations (28), (30), (31), and (32). Also shown are the simulation data for $\rho_L(k)$. The error bars are of the order of the symbol sizes. For $\alpha = \alpha_c$ the simulation results are indistinguishable from the theoretical straight line (33). However, for $\alpha \neq \alpha_c$ there is a small but definite discrepancy between the theory and the simulation data. We attribute this discrepancy to the approximate nature, mentioned above, of the master equation (23) on which the theory is based. Finding a theoretical description more accurate than (23) is at this moment an open challenge.

5.4. Critical region

Near criticality we may expand (28) in powers of $\Delta\alpha = \alpha - \alpha_c$ and obtain to leading order

$$\xi \simeq -\frac{\alpha_c^2}{J^F \Delta\alpha} = -\frac{1+a_c}{a_c} \frac{\alpha_c^2}{\Delta\alpha}. \quad (34)$$

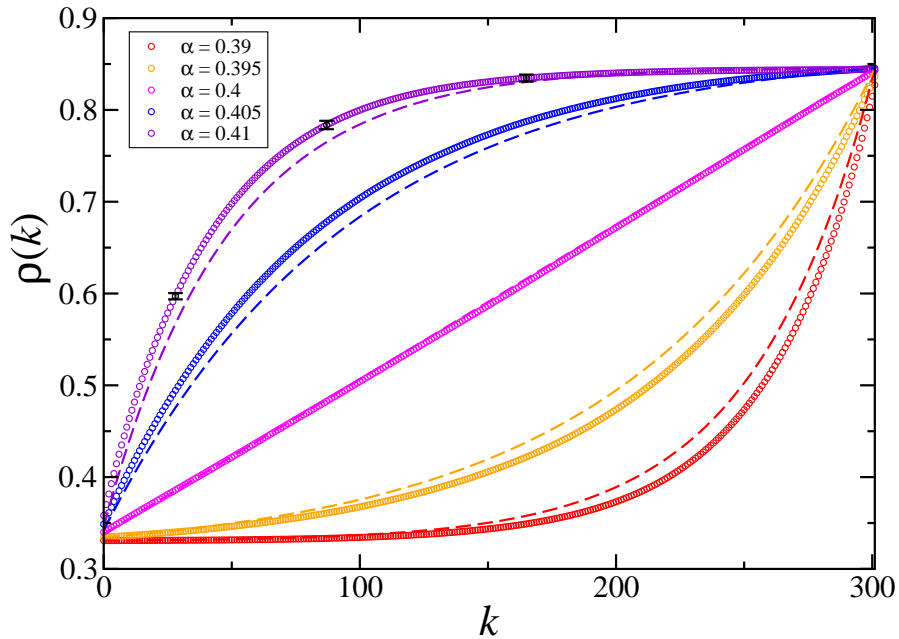


Figure 6. Spatial density profiles as a function of the lattice site index k in a system of length $L = 300$. The exit probability is $\beta = 0.4$ and the entrance probabilities α are close to the critical value $\alpha_c = 0.4$. The data points join together to produce heavy solid curves. A few error bars are given for the case $\alpha = 0.41$. For all curves the error bars are of the order of the symbol sizes. Each simulation had a duration of 8×10^7 time steps. Dashed curves: the theoretical predictions according to equations (28), (30), (31), and (32).

To lowest order in $\Delta\alpha$ we have $\rho^J \simeq \rho^F/\alpha_c$ and thus the density profile (30) becomes

$$\begin{aligned} \rho_L(k) &\simeq \frac{\rho^F}{\alpha_c} \left[1 + (\alpha_c - 1) \frac{1 - e^{-(L-k)/\xi}}{1 - e^{-L/\xi}} \right] \\ &= \frac{a_c}{(1 + a_c)(1 - e^{-a_c})} \left[1 - e^{-a_c} \frac{1 - e^{-(L-k)/\xi}}{1 - e^{-L/\xi}} \right]. \end{aligned} \quad (35)$$

5.5. Scaling limit

We shall now consider (35) in the scaling limit $\Delta\alpha \rightarrow 0$ and $L \rightarrow \infty$ with $\Delta\alpha L$ fixed. In this limit the density profile $\rho_L(k)$ becomes a function of the single ratio k/L , as one may see by combining (35) and (34), and noticing that the variable z defined by

$$z = \lim_{\substack{\alpha \rightarrow \alpha_c \\ L \rightarrow \infty}} \frac{L}{\xi} = -\frac{a_c}{1 + a_c} \frac{\Delta\alpha L}{\alpha_c^2} \quad (36)$$

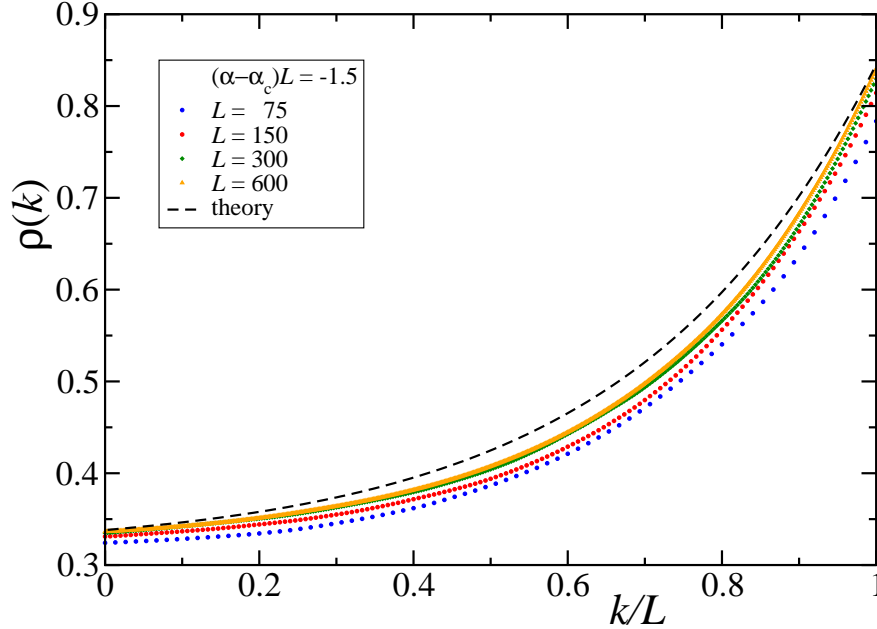


Figure 7. Spatial density profiles as a function of the scaled lattice site index k/L , obtained from Monte Carlo simulations for various system sizes L and various α values, with $(\alpha - \alpha_c)L = -1.5$ fixed. In the scaling limit the simulation data converge to a profile that is seen to depend only on k/L , as predicted by the domain wall theory. Dashed curve: the domain wall theoretical prediction for the density profile in the scaling limit. The exit probability $\beta = 0.4$ is fixed.

has a fixed value. In this limit the profile (35) may be simplified to

$$\rho_L(k) = \frac{a_c}{1 + a_c} \left[1 + \frac{1 - \alpha_c e^{-z(1-k/L)} - e^{-z}}{\alpha_c (1 - e^{-z})} \right] \quad (37)$$

which depends only on the two scaling variables z and k/L . This scaling behavior of the profile is confirmed by the simulation data shown in figure 7: for increasing L the profiles converge to a limit curve. The limiting curve of the simulation data again exhibits a slight deviation from the theoretical curve (37).

We return now to figure 5 and explain, again in the same scaling limit, the finite size effects observed there. In order to obtain the space averaged density we have to determine the mean value of the profile (37) over $0 \leq k/L \leq 1$. The result is that we obtain for the L and $\Delta\alpha$ dependent space averaged particle density ρ the scaling expression

$$\rho = \rho_c^J - (\rho_c^F - \rho_c^J)\Psi(z) \quad (38)$$

with $-\infty < z < \infty$ and the scaling function Ψ given by⁺

$$\Psi(z) = 1 + \frac{1}{z} - \frac{1}{1 - e^{-z}}. \quad (39)$$

Monte Carlo simulations were carried out on systems of different sizes L . We have seen in figure 6 that exactly at the critical point $\alpha = \alpha_c$ the simulated profile is linear for all system sizes; as a consequence, in figure the space averaged density coincides for $\Delta\alpha L = 0$ within error bars with the theoretical value. Within distance L^{-1} from criticality the transient time necessary to reach stationarity grows with L and we had to make sure that the data represent true stationary state values. The simulated system sizes L in figure 8 are therefore smaller than the largest values shown in figure 5. The Monte Carlo data in figure 8 confirm the validity of the scaling as a function of the product variable $(\alpha - \alpha_c)L$.

As in figure 7, the Monte Carlo curves in figure 8 converge, when L increases, to a limit curve. Again, there is a slight but significant difference between the theoretical limit function and the simulation data, a consequence pointed out above of the fact that the domain wall theory is only approximate here.

6. Conclusion

Motivated by the modeling of pedestrian motion, we have in this paper pursued our study of a new ‘frozen shuffle’ update scheme for the totally asymmetric exclusion process (TASEP) on a one-dimensional lattice. An advantage of this scheme is that it fixes deterministic rules of priority when two hard-core particles attempt to hop to the same target site, a feature that allows for more efficient Monte-Carlo simulations. This is in contrast with the widely used parallel update which, when two pedestrians want to hop to the same site, generates conflicts which have to be solved by extra ad-hoc rules. Actually these algorithmic conflicts may have a physical counterpart: In dense crowds conflicts between real interacting pedestrians are thought to be one of the sources for the clogging effect observed near exits in emergency evacuation [3]. However, it is still an open question to determine whether the effect of the conflicts due to parallel update is overestimated or not, compared to the effect of real-life conflicts between pedestrians. Shuffle update yields an alternative that solves conflicts in a smoother way and may be more appropriate for pedestrian modelling in particular when the density is not too high. Besides, this scheme is easily accessible to analytical study.

Compared to other update schemes, the frozen shuffle update modifies the properties of the stationary state in the closed system studied in reference [9] as well as in the open system studied here. The open system, just like the closed one, appears capable of sustaining ‘free flow’ and ‘jammed’ states. More specifically, the jammed

⁺ The similarity of this expression to (15) is probably a coincidence.

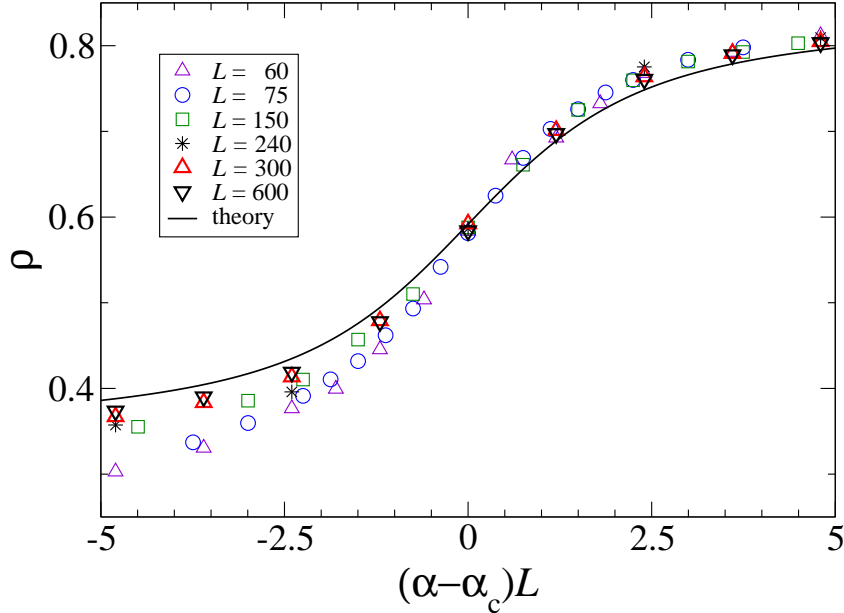


Figure 8. Space averaged particle density for various system sizes L , as a function of the scaling variable $(\alpha - \alpha_c)L$. Solid curve: the theoretical scaling function according to equations (38), (39), and (36), which describes the finite size rounding of the transition seen in figure 5. The Monte Carlo data are for $\beta = 0.4$, hence $\alpha_c = 0.4$. For increasing L they converge to a scaling function whose deviation from the theoretical prediction is very small but nevertheless statistically significant.

state's behavior is fully driven by the platoon structure, where platoons are ensembles of neighbor particles that move as a whole at each time step. As the platoon structure depends on the injection procedure, the flux of the jammed phase for the frozen shuffle update (in contrast to other update schemes) depends not only on the exit probability β but also on the entrance probability α .

In spite of this specificity, the transition line between the free flow and the jammed phase is found to be the usual $\alpha = \beta$ line. As we considered only the deterministic version of the model (particles move forward with probability 1 when the target site is empty), there is no maximal current phase. It could be of interest to extend the study to the case of particles hopping with probability $p < 1$.

We have accompanied our theoretical results by Monte Carlo simulations. and found excellent agreement for the phase diagram.

Finally, in order to explain the finite system size effects observed in the Monte Carlo simulations and especially important near the transition, we have applied a domain wall approach originally developed in references [15, 16, 17, 18, 19]. Frozen shuffle

update with deterministic dynamics leads to the remarkable property that the position of the domain wall that separates two homogeneous regions can be determined at the microscopic scale of the lattice distance. The domain wall theory appears to account quite well for the finite size effects, but we point out that nevertheless a small but definite discrepancy persists between this theory and the simulation data. The discrepancy concerns in particular the wall localization length, near the border of the system, for reasons still to be understood.

An update scheme related to ours and preceding it, called ‘random shuffle’ update, has been proposed [5, 7] for the improvement of pedestrians models. That scheme has no obvious interpretation in terms of the interaction between pedestrians and should rather be viewed as an algorithm devised just to avoid conflicts. By contrast, the ‘frozen shuffle’ variant presented in this paper has a physical interpretation in terms of phase differences in the stepping cycle, which makes it relevant for applications to pedestrians.

In forthcoming work [20] we will study the case of two intersecting lanes of pedestrians (TASEPs) simulated with frozen shuffle update.

- [1] C. Burstedde, K. Klauck, A. Schadschneider, and J. Zittartz. Simulation of pedestrian dynamics using a 2-dimensional cellular automaton. *Physica A*, 295:507–525, 2001.
- [2] A. Schadschneider. Cellular automaton approach to pedestrian dynamics - theory. In M. Schreckenberg and S.D. Sharma (Eds.), editors, *Pedestrian and Evacuation Dynamics*, pages 75–85. Springer, 2002.
- [3] A. Kirchner, K. Nishinari, and A. Schadschneider. Friction effects and clogging in a cellular automaton model for pedestrian dynamics. *Phys. Rev. E*, 67:056122, 2003.
- [4] H. Klüpfel. The simulation of crowds at very large events. In A. Schadschneider, T. Poschel, R. Kuhne, M. Schreckenberg, and D.E. Wolf, editors, *Traffic and Granular Flow '05*, pages 341–346, 2007.
- [5] M. Wölki, A. Schadschneider, and M. Schreckenberg. Asymmetric exclusion processes with shuffled dynamics. *J. Phys. A-Math. Gen.*, 39:33–44, 2006.
- [6] M. Wölki, A. Schadschneider, and M. Schreckenberg. In: N. Waldau, P. Gattermann, H. Knoflacher, and M. Schreckenberg (editors), *Pedestrian and Evacuation Dynamics 2005*, p. 423-428, Springer (Berlin) 2007.
- [7] D.A. Smith and R.E. Wilson. Dynamical pair approximation for cellular automata with shuffle update. *J. Phys. A: Math. Theor.*, 40(11):2651–2664, 2007.
- [8] D. Chowdhury, A. Schadschneider, and K. Nishinari. Physics of transport and traffic phenomena in biology: from molecular motors and cells to organisms. *Physics of Life Reviews*, 2:318–352, 2005.
- [9] C. Appert-Rolland, J. Cividini, and H.J. Hilhorst. Frozen shuffle update for an asymmetric exclusion process on a ring. *To appear in JSTAT. Preprint arXiv:1105.0352*.
- [10] G. Schütz and E. Domany. Phase transitions in an exactly soluble one-dimensional exclusion process. *J. Stat. Phys.*, 72:277–296, 1993.
- [11] B. Derrida, M.R. Evans, V. Hakim, and V. Pasquier. Exact solution of a 1d asymmetric exclusion

- model using a matrix formulation. *J. Phys. A*, 26:1493, 1993.
- [12] J. de Gier and B. Nienhuis. Exact stationary state for an asymmetric exclusion process with fully parallel dynamics. *Phys. Rev. E*, 59:4899–4911, 1999.
 - [13] N. Rajewsky, L. Santen, A. Schadschneider, and M. Schreckenberg. The asymmetric exclusion process: Comparison of update procedures. *J. Stat. Phys.*, 92:151, 1998.
 - [14] B. Derrida, J.L. Lebowitz, and E.R. Speer. Shock profiles for the asymmetric simple exclusion process in one dimension. *J. Stat. Phys.*, 89:135–167, 1997.
 - [15] A.B. Kolomeisky, G.M. Schütz, E.B. Kolomeisky, and J.P. Straley. Phase diagram of one-dimensional driven lattice gases with open boundaries. *J. Phys. A: Math. Gen.*, 31:6911, 1998.
 - [16] C. Pigorsch and G.M. Schütz. Shocks in the asymmetric simple exclusion process in a discrete-time update. *J. Phys. A: Math. Gen.*, 33:7919–7933, 2000.
 - [17] M. Dudziński and G.M. Schutz. Relaxation spectrum of the asymmetric exclusion process with open boundaries. *J. Phys. A: Math. Gen.*, 33:8351, 2000.
 - [18] Z. Nagy, C. Appert, and L. Santen. Relaxation times in the ASEP model using a DMRG method. *J. Stat. Phys.*, 109:623–639, 2002.
 - [19] L. Santen and C. Appert. The asymmetric exclusion process revisited: Fluctuations and dynamics in the domain wall picture. *J. Stat. Phys.*, 106:187–199, 2002.
 - [20] C. Appert-Rolland, J. Cividini, and H.J. Hilhorst. Frozen shuffle update for intersecting traffic lanes. *In preparation*, 2011.